Chinese Journal of Natural Medicines

Natural medicine can substitute antibiotics in animal husbandry: protective effects and mechanisms of rosewood essential oil against *Salmonella* infection

Lanqiao WANG, Juan FANG, Heng WANG, Baoyu ZHANG, Nan WANG, Xinyu YAO, He LI, Jiazhang QIU, Xuming DENG, Bingfeng LENG, Jianfeng WANG, Wenxi TAN, Qiaoling ZHANG

Citation: Lanqiao WANG, Juan FANG, Heng WANG, Baoyu ZHANG, Nan WANG, Xinyu YAO, He LI, Jiazhang QIU, Xuming DENG, Bingfeng LENG, Jianfeng WANG, Wenxi TAN, Qiaoling ZHANG, Natural medicine can substitute antibiotics in animal husbandry: protective effects and mechanisms of rosewood essential oil against *Salmonella* infection, Chinese Journal of Natural Medicines, 2024, 22(9), 785−796. doi: 10.1016/S1875−5364(24)60576−5.

View online: https://doi.org/10.1016/S1875−5364(24)60576−5

Available online at www.sciencedirect.com
ScienceDirect
Chinese Journal of Natural Medicines 2024, **22**(9): 785-796
doi: 10.1016/S1875-5364(24)60576-5
Chinese Journal of Natural Medicines

•Original article•

Natural medicine can substitute antibiotics in animal husbandry: protective effects and mechanisms of rosewood essential oil against *Salmonella* infection

WANG Lanqiao[1], FANG Juan[1], WANG Heng[1], ZHANG Baoyu[1], WANG Nan[1], YAO Xinyu[1], LI He[1], QIU Jiazhang[1], DENG Xuming[1], LENG Bingfeng[2], WANG Jianfeng[1], TAN Wenxi[3*], ZHANG Qiaoling[1*]

[1] *State Key Laboratory for Diagnosis and Treatment of Severe Zoonotic Infectious Diseases, Key Laboratory for Zoonosis Research of the Ministry of Education, Institute of Zoonosis, and College of Veterinary Medicine, Jilin University, Changchun 130062, China;*
[2] *Shenzhen Beichen Biotech Co., Ltd., Shenzhen 518057, China;*
[3] *Department of Obstetrics and Gynecology, The Second Hospital of Jilin University, Changchun 130041, China*

Available online 20 Sep., 2024

[ABSTRACT] *Aniba rosaeodora* essential oil (RO) has been traditionally used in natural medicine as a substitute for antibiotics due to its notable antidepressant and antibacterial properties. *Salmonella*, a prevalent pathogen in foodborne illnesses, presents a major challenge to current antibiotic treatments. However, the antibacterial efficacy and mechanisms of action of RO against *Salmonella* spp. remain underexplored. This study aims to elucidate the chemical composition of RO, evaluate its antibacterial activity and mechanisms against *Salmonella in vitro*, and further delineate its anti-inflammatory mechanisms *in vivo* during *Salmonella* infection. Gas chromatography-mass spectrometry (GC-MS) was utilized to characterize the chemical constituents of RO. The antibacterial activity of RO was assessed using minimal inhibitory concentration (MIC) and time-kill assays. Various biochemical assays were employed to uncover the potential bactericidal mechanisms. Additionally, mouse and chick models of *Salmonella* infection were established to investigate the prophylactic effects of RO treatment. RO exhibited significant antibacterial activity against both Gram-positive and Gram-negative bacteria, with an MIC of 4 mg·mL^{-1} for *Salmonella* spp. RO treatment resulted in bacterial damage through the disruption of lipid and purine metabolism. Moreover, RO reduced injury and microbial colonization in infected mice and chicks. RO treatment also modulated the host inflammatory response by inhibiting proinflammatory pathways. In conclusion, our findings demonstrate that RO is effective against *Salmonella* infection, highlighting its potential as an alternative to antibiotics for antibacterial therapy.

[KEY WORDS] Rosewood essential oil; *Salmonella*; *Aniba rosaeodora*; Antibacterial effect; Anti-inflammation; Anti-infection
[CLC Number] R965 **[Document code]** A **[Article ID]** 2095-6975(2024)09-0785-12

Introduction

Species of the *Salmonella* genus are the leading cause of human fatalities from foodborne diseases globally, posing a significant public health challenge [1]. *Salmonella typhimurium* (*S. Tm*), a serotype of *Salmonella*, shows extensive horizontal and vertical transmission across various animals, including rodents, wild birds, foxes, and free-range egg-laying chicks [2]. Given that poultry is one of the most widely consumed meats worldwide, it can harbor pathogens such as *S. pullorum* (*SP*), which poses considerable risks to animal husbandry and the food industry [3]. The intensive farming of poultry has led to the widespread misuse of antibiotics to prevent and treat diseases, resulting in increased bacterial resistance. Research by Zhang indicates that antibiotic misuse in perinatal medicine ranges from 50% to 70% [4]. This unreasonable antibiotic abuse across industrial, residential, and agricultural sectors is expanding the environmental resistome [5]. The limited and inappropriate use of antibiotics can lead to increased *Salmonella* tolerance over time [6]. Therefore, there

[Received on] 03-Dec.-2023
[Research funding] This work was supported by the National Key Research and Development Program of China (No. 2021YFD 1801000), the National Natural Science Foundation of China (Nos. 31772798, 31970507, 81861138046, and 31902321).
[*]**Corresponding author]** E-mails: tanwenxi1981@163.com (TAN Wenxi); zql@jlu.edu.cn (ZHANG Qiaoling)
These authors have no conflict of interest to declare.

is an urgent need for alternative treatments for *Salmonella* infections.

In the context of widespread antibiotic abuse, increasing evidence suggests that natural products (NPs) can serve as effective alternatives in animal husbandry and aquaculture for infection control [7]. Essential oils, a category of NPs, offer various benefits, including enhanced immunity, antioxidation, and antibacterial activity through multiple mechanisms [8]. For example, thymol oil reduces intracellular ATP levels to combat *Cronobacter sakazakii*, while basil oil stimulates reactive oxygen species (ROS) to achieve antibacterial effects [9, 10]. Due to their high safety and natural purity, essential oils are increasingly being used in practical applications over antibiotics. Oregano oil has been shown to effectively prevent bacterial infections and maintain intestinal health in broilers compared to sulfated colistin [11]. Similarly, rosemary oil can replace avilamycin to improve broiler growth performance [12]. Thus, essential oils derived from traditional medicinal plants are promising natural antibacterial agents that can replace antibiotics.

Aniba rosaeodora (Rosewood), a member of the Lauraceae family, is a large tree reaching up to 25 meters in height. It is recorded in the World Flora Online (WFO) and *Compendium of Materia Medica* for its disinfection and analgesic effects. Rosewood, found in the Amazon region and southern China, exhibits various pharmacological activities, including stasis removal, pain alleviation, and antiviral effects [13]. Rosewood essential oil (RO) is one of the most valuable NPs derived from this tree. As a volatile oil, RO is widely used for traditional medical purposes due to its anti-anxiety, sedative, and anticonvulsant effects [14, 15]. In various epilepsy models, RO has been shown to suppress seizures through the inhibition of cAMP [16]. However, few studies have explored the antibacterial properties of RO, aside from its calming effects. This study aims to discover new traditional natural agents against bacterial infections and elucidate the antibacterial mechanisms of RO. We investigate the potential antibacterial efficacy of RO against *Salmonella*, focusing on bacterial targeting and the impact of RO on the inflammatory response based on host targeting. Our results pave the way for developing essential oils as alternatives to antibiotics and antibacterial agents in clinical settings.

Materials and Methods

Bacterial strains, reagents, and materials

The bacterial strains used in this study included *Salmonella* strains (SL1344, SP0114, ATCC14028, HYM2, GP-9, and CVCC1789), *Escherichia coli* strains (ATCC25922, 487, ZJ02, and K88), *Acinetobacter baumannii* ATCC17978 and *Klebsiella pneumoniae* Rosetta were stored in our laboratory. These strains were stored in our laboratory at –80 °C in 40% glycerol. Prior to experiments, all strains were revived in Luria–Bertani (LB) broth (Qingdao Hope Biol-Technology, Co., Ltd.) and cultured at 37 °C with shaking at 200 r·min^{-1} for 16 h.

RO was procured from Ji'an Zhongxiang Natural Vegetable Essential Oil Co., Ltd. (Jilin, China), and was diluted with dimethyl sulfoxide (DMSO, Sigma) and stored at 4 °C until use.

GC-MS/MS analysis of RO ingredients

The chemical composition of RO was analyzed using a Trace DSQ II GC-MS system (Thermo Fisher Scientific, USA). The analytes were separated on a DB-5 ms silica-based capillary column (30 m × 0.25 mm, 0.25 μm film thickness). Helium was used as the carrier gas at a constant flow rate of 1.2 mL·min^{-1}. A 1 μL sample was injected in splitless mode. The electron ionization (EI) energy was set to 70 eV for optimal ionization. The ion source temperature was maintained at 220 °C, and the interface temperature was set at 280 °C. The mass spectrometer scanned a range from 60 to 600 atomic mass units (amu) to identify the components present in the RO.

Minimal inhibitory concentration (MIC), minimum bactericidal concentration (MBC), and bacteriostatic zone (DIZ) assays

The MIC, MBC, and DIZ assays were conducted as previously described [17]. To determine the MIC, diluted RO was added to sterile LB broth to achieve final concentrations ranging from 8 mg·mL^{-1} to 8 μg·mL^{-1}. An overnight bacterial culture was then introduced into the LB broth containing RO to reach a final concentration of 5 × 10^5 colony-forming units (CFU)/mL, and the MIC was defined as the lowest concentration that inhibited visible bacterial growth after 16 h. For the MBC determination, 2 μL samples from each well without visible growth in the MIC test were plated on LB agar (Agar, Sigma), and was established as the lowest concentration at which no bacterial colonies were observed. In the DIZ assay, 20 μL of RO was added to wells in agar plates inoculated with bacteria. And the diameter of the inhibition zones (DIZ) was measured.

Bacterial growth analysis and time-kill assay

Salmonella typhimurium SL1344 and *Salmonella pullorum* SP0114 were cultured in LB broth with varying concentrations of RO (0, ½ MIC, MIC, and 2 × MIC) at 37 °C with shaking at 200 r·min^{-1}. The bacterial growth was monitored by measuring the optical density at 600 nm at intervals of 0, 2, 4, 6, 8, and 10 h. Additionally, a time-kill assay was performed by co-culturing *Salmonella* (5 × 10^5 CFU/mL) with the same RO concentrations at 37 °C. Bacterial samples from each condition were plated on LB agar, and the number of colonies was counted.

Detection of RO-induced bacterial injury

The extent of bacterial injury induced by RO at above concentrations was assessed using the Live/Dead BacLight Bacterial Viability Kit (Invitrogen). Stained bacterial cells were observed under an inverted fluorescence microscope (Olympus, Tokyo).

Analysis of bacterial membrane homeostasis

SP0114 and SL1344 were treated with RO at concentra-

tions of 0, ½ MIC, and MIC in LB culture medium for 4 h. After treatment, the bacteria were collected, fixed with a stationary solution (Servicebio, China), freeze-dried, and observed using scanning electron microscopy (SEM). The leakage of nucleic acids and proteins from RO-treated *Salmonella* was measured at intervals of 0, 1, 3, 5, 7, and 9 h [18]. Absorbance was recorded at $OD_{260\ nm}$ for nucleic acids and $OD_{280\ nm}$ for proteins, as previously described.

Fluorescence intensity measurements of nonprotein nitrogen (NPN) and propidium iodide (PI) in SP0114 and SL1344 treated with 0, ½ MIC, MIC, and 2 × MIC RO were performed at 0, 4, 8, and 12 h, based on established methods [19]. Additionally, DAPI/PI staining of SL1344 treated with 0, ½ MIC, MIC, and 2 × MIC RO was conducted to qualitatively assess membrane integrity, following the protocol described in previous research [20].

Assessment of bacterial intracellular metabolic homeostasis

Salmonella typhimurium SL1344 was treated with RO at above four concentrations for the quantitative detection of ROS and adenosine triphosphate (ATP) levels. Post-treatment, the bacteria were resuspended in PBS, and ROS levels were measured using a fluorescence assay kit (S0033S, Beyotime, China) with a fluorescent enzyme marker. ATP levels were quantified at 4, 8, and 12 h post-treatment using a mitochondrial-specific fluorescent dye (Sigma, China) according to established protocols [21]. Additionally, ROS fluorescence images were captured qualitatively following previously described methods [22].

Metabolomics analysis

Salmonella typhimurium SL1344 in the logarithmic growth phase was treated with RO at 0 (control) and MIC concentrations for 2 h at 37 °C. The samples were then rapidly frozen in liquid nitrogen and stored at −80 °C. Metabolite detection was performed using UHPLC-MS/MS analysis on a Vanquish UHPLC system (Thermo Fisher, Germany) coupled with an Orbitrap Q Exactive™ HF mass spectrometer (Thermo Fisher, Germany) at Novogene Co., Ltd. (Beijing, China). Metabolites and pathway enrichment analyses were conducted using the KEGG (Kyoto Encyclopedia of Genes and Genomes) database.

The detection of hydrogen peroxide (H_2O_2) treated with or without RO was carried out using the Hydrogen Peroxide Assay Kit (S0038, Beyotime, China) and the Hydroxyl Free Radical Assay Kit (A018-1-1, Nanjing Jiancheng, China), respectively.

Animal experiments

The animal experiments conducted in this study were approved by the Institutional Animal Care and Use Committee of Jilin University (permit number SY202306059).

To establish *Salmonella* infection models, female BALB/c mice (aged 6 to 8 weeks) were obtained from Liaoning Changsheng Biotechnology Co., Ltd. (Liaoning, China). Each mouse was gavaged with either 1×10^7 CFU (sublethal dose) or 5×10^7 CFU (lethal dose) of *Salmonella* [23]. For the chick model, 1-day-old male Hyline-brown healthy chicks (Jilin Academy of Agricultural Sciences, Changchun, China) were gavaged with either 1×10^{10} CFU (sublethal dose) or 1×10^{11} CFU (lethal dose) of *Salmonella*. Both mice and chicks were pre-treated with RO 2 hours before the *Salmonella* challenge. The RO was administered at dosages of 40 $mg \cdot kg^{-1}$ (low dose, $n = 5$), 80 $mg \cdot kg^{-1}$ (medium dose, $n = 5$), and 160 $mg \cdot kg^{-1}$ (high dose, $n = 5$). Subsequently, RO was administered *via* gavage every 24 h for 5 d in mice and 4 d in chicks. The healthy control group and the untreated control group (infected animals without RO treatment) received the solvent vehicle (carboxymethylcellulose, CMC-Na) on the same schedule. The mice and chicks were euthanized 5 and 4 d post-infection, respectively. Tissue samples from the liver, spleen, cecum, and colon were collected and plated onto Xylose Lysine Deoxycholate (XLD) agar (Qingdao Hope Biol-Technology Co., Ltd.), followed by incubation at 37 °C. Additionally, portions of the target organs from each group were fixed in a 4% formaldehyde solution (Sigma). After dehydration, embedding, and sectioning, hematoxylin-eosin staining was performed to observe the histopathology.

Enzyme-linked immunosorbent (ELISA) assay

The levels of cytokines, including tumor necrosis factor-α (TNF-α), interleukin 6 (IL-6), interleukin 1β (IL-1β), interleukin 10 (IL-10), and interferon-γ (IFN-γ), in tissue samples were measured by enzyme-linked immunosorbent assay kits (eBioscience, USA).

Real-time fluorescence quantitative PCR (qRT-PCR) analysis

To investigate the effect of RO on inflammatory signaling pathways *in vivo*, total RNA was extracted from the liver tissues of mice and chicks. Primer sequences for target genes were designed using SnapGene software (PREMIER Biosoft International, USA) (see Supplement Table 1). The relative expression levels of target genes were quantified by the M5 HiPer SYBR Premix EsTaq kit (Mei5 Biotechnology, Co., Ltd.) and calculated using the $2^{-\triangle\triangle Ct}$ method, normalized to the reference gene GAPDH.

Protein extraction and Western blotting analysis

Protein extraction samples were performed on 50 mg liver tissue in each group for following analysis. For WB analysis, 20 μg of total protein per sample was separated and then transferred to a PVDF membrane. The membranes were blocked,followedbyincubationwithprimaryantibodiesovernight (Supplement Table 2). The membranes were washed with Tris-buffered saline with Tween-20 (TBST) and then incubated with an anti-rabbit secondary antibody (1 ∶ 3000). After additional washes with TBST, the membranes were developed by enhanced chemiluminescence (ECL) reagent (Kangwei Reagent Co., Ltd., Beijing, China). All antibodies were obtained from Biotec, Beijing, China. *β*-Actin was used as the internal reference protein. The greyscale values of the bands were analyzed using Image J software (National Institutes of Health, Bethesda, MD).

Statistical analysis

Data were collected from at least three independent biological replicates and analyzed using GraphPad Prism soft-

ware. Statistical significance was determined using t-tests and ANOVA. Data are presented as mean ± SD, with *P*-values below 0.05 or 0.01 considered statistically significant. ($^{*}P < 0.05$; $^{**}P < 0.01$).

Results

GC-MS/MS analysis of the chemical constituents of RO

The chemical composition of RO was analyzed using GC-MS. The analysis identified a total of 18 components, which together accounted for 98.4% of the total composition of RO (see Supplement Table 3 and Supplement Fig. 1). The primary constituent was linalool, making up 59.60% of the oil. Other significant components included ethyl propionate (31.23%), eucalyptol (2.42%), and dextrose camphor (2.09%). These findings indicate that linalool, ethyl propionate, eucalyptol, and dextrose camphor are the major constituents of RO, collectively constituting 95.34% of the oil's composition.

RO effectively restrained the proliferation of Salmonella

The antibacterial activity of RO against *Salmonella* and other bacteria was evaluated. As detailed in Supplement Table 4, the diameters of inhibition zones (DIZs) for all tested microorganisms were not less than 13.5 mm, indicating moderate sensitivity to 8 mg of RO per well. Notably, the DIZs for SL1344 and SP0114 were 14.0 ± 0.6 mm and 19.7 ± 0.5 mm, respectively, classifying these strains as sensitive to RO. The antibacterial efficacy of RO was further quantified using MIC and MBC assays. RO exhibited effective bacteriostatic and bactericidal activities against all tested bacteria. The MICs and MBCs for all *Enterobacteriaceae* strains ranged from 2.0 to 8.0 mg·mL^{-1}. For *Staphylococcus aureus*, the MIC and MBC were 4.0 and 8.0 mg·mL^{-1}, respectively. For both SL1344 and SP0114, RO displayed bactericidal effects, with MBC/MIC ratios not exceeding 4 (Supplement Table 4).

To investigate the effect of RO on the growth of SL1344 and SP0114, bacterial cultures were monitored over a 10-hour period. Figs. 1A and 1B show that untreated *Salmonella* exhibited typical growth patterns, while RO treatment inhibited bacterial growth in a concentration-dependent manner. No bacterial growth was observed in samples treated with MIC and 2 × MIC concentrations of RO. The bactericidal kinetics of RO were assessed using a time-kill assay (Figs. 1C and 1D), plotting the logarithmic values of CFU·mL^{-1}. MIC-level RO treatment significantly reduced SL1344 and SP0114 counts within the first 3 h. For both strains treated with 2 × MIC RO, bacterial counts decreased from $1 \times 10^{6.5}$ CFU·mL^{-1} to 0 within 1 h. Furthermore, live-dead bacterial staining was conducted to observe the impact of RO on SL1344 (Fig. 1E). Untreated SL1344 showed green fluorescence, indicating live cells, while RO-treated bacteria exhibited varying degrees of red fluorescence, indicating cell death, in a dose-dependent manner. In summary, our findings demonstrate that RO is a potent bactericidal agent against *Salmonella*, with significant inhibitory effects on bacterial growth and viability.

RO disturbed the cell membrane homeostasis of Salmonella

To elucidate the mechanism by which RO acts against *Salmonella*, we examined bacterial morphology under SEM following RO treatment. As shown in Fig. 2A, untreated *Salmonella* exhibited a short rod-shaped structure with intact morphology and a smooth surface. In contrast, both SL1344 and SP0114 treated with RO displayed significant morphological changes, including cell structure disruption, indicating that RO treatment disturbs the membrane homeostasis of *Salmonella*. We further investigated membrane damage by measuring the leakage of nucleic acids and proteins. As expected, RO treatment caused a sharp increase in protein (Fig. 2B) and nucleic acid (Fig. 2C) leakage within 1 h, which then fluctuated within a certain range. A dose-dependent pattern of RO-mediated leakage of nucleic acids and proteins was observed from the 1st to the 24th h. (Figs. 2B and Fig. 2C). To further examine the disruption of *Salmonella* homeostasis, DAPI/PI staining assays were performed (Fig. 2D). RO treatment resulted in an increase in red fluorescence, indicating decreased bacterial membrane integrity and increased permeability, with a clear concentration dependence. We also assessed the luminescence intensity of NPN, a reagent that fluoresces upon binding to hydrophobic sites on the cell membrane, and PI at 0, 4, and 8 h. The fluorescence intensity of both NPN and PI increased with RO treatment in a concentration- and time-dependent manner (Figs. 2E and 2F). These results indicated that RO treatment enhances bacterial membrane permeability, promoting substance entry and the leakage of nucleic acids and proteins. In summary, our findings suggest that RO significantly disrupts the cell membrane homeostasis of *Salmonella*, increasing membrane permeability and causing leakage of essential cellular components.

RO induced the disarray of intracellular metabolic homeostasis

Given the disruption of membrane homeostasis in *Salmonella* by RO, we further investigated its impact on intracellular metabolic processes. As depicted in Fig. 3A, intracellular ATP levels were significantly depleted following RO treatment, although this depletion did not show a time-dependent pattern. The expression of ATP-related genes (*atpH*, *atpG*, *atpC*, *msbA*, and *mdlB*) was significantly elevated, with at least a twofold increase compared to untreated samples. The addition of RO increased the expression by at least twofold compared with that of the samples without RO (Fig. 3B). The activation of atpC, in particular, suggests a self-protective mechanism in response to RO-induced stress. ROS-related fluorescence imaging revealed that the RO-treated group exhibited a markedly higher fluorescence intensity compared to the untreated wild-type (WT) group under the same exposure conditions (Fig. 3C). This increase in fluorescence was quantitatively confirmed using a microplate reader, showing a concentration-dependent rise in ROS levels with RO treatment (Fig. 3D). Further analysis of ROS-associated

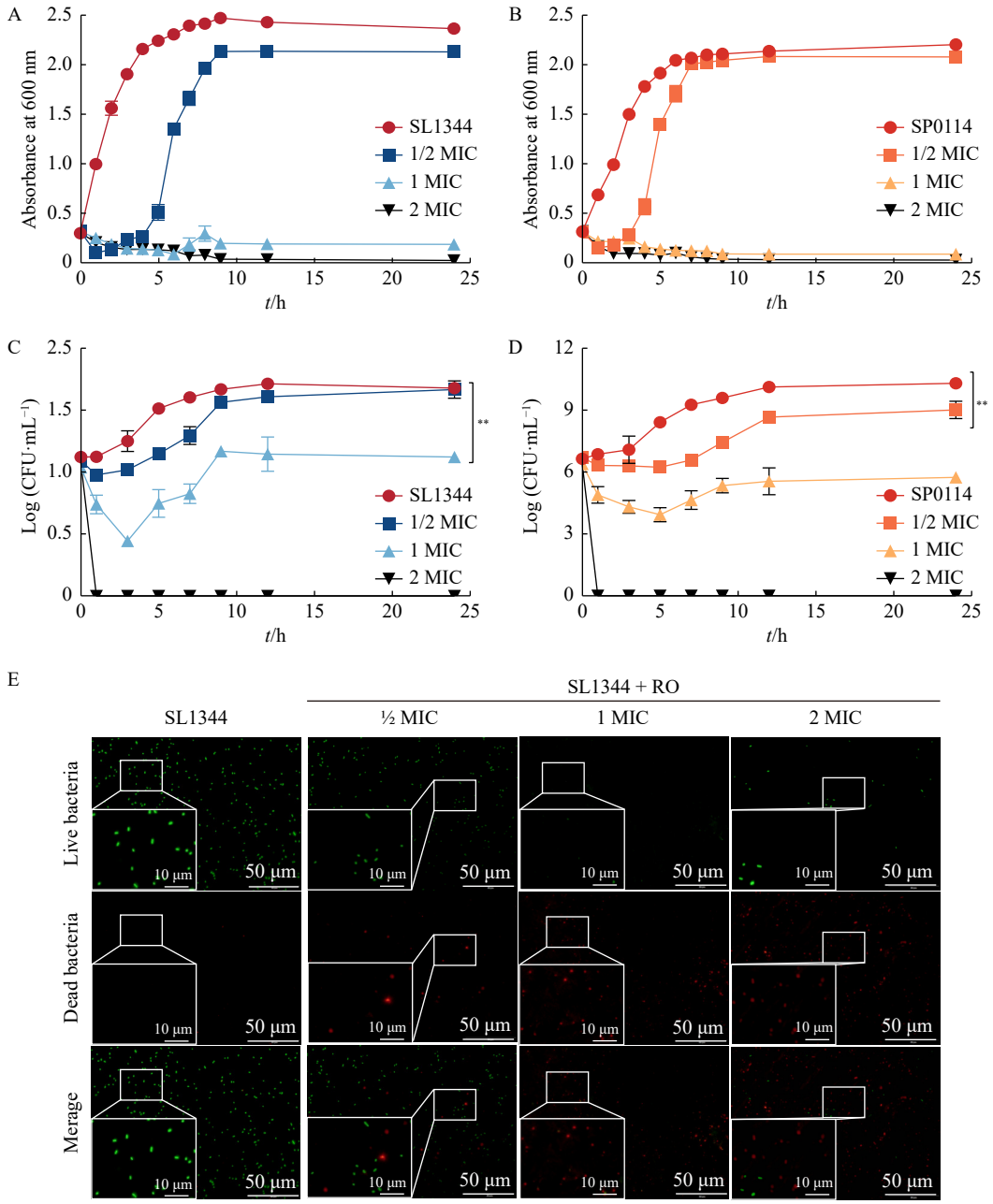

Fig. 1 RO effectively restrained *Salmonella* proliferation *in vitro*. Absorbance was monitored at 600 nm at 0, 1, 2, 3, 4, 5, 6, 7, 8, 9, 12, and 24 h of *S. typhimurium* SL1344 (A) and *S. pullorum* SP0114 (B) treated with RO at concentrations of 0, ½ MIC, MIC, and 2 × MIC. Time-kill assay of SL1344 (C) and SP0114 (D) with above RO at 0, 1, 3, 5, 7, 9, 12, and 24 h. (E) Images representing the states of SL1344 with the indicated concentrations of RO are shown at 600 × magnification. The left row and middle row indicate live bacteria with green fluorescence and dead bacteria with red fluorescence, respectively.

genes (*uspA*, *uspB*, and *uspC*) and outer membrane protein (omp) family genes (*ompA*, *ompB*, *ompC*, *ompR*, and *ompF*) in *Salmonella* showed significant upregulation of all ROS-associated genes following RO treatment (Fig. 3E). Among the omp genes, *ompA*, *ompB* and *ompC* were upregulated, while *ompR* and *ompF* were downregulated in response to RO (Fig. 3F). In conclusion, our findings suggest that RO disrupts intracellular metabolic homeostasis in *Salmonella* by depleting ATP levels and inducing ROS overproduction, thereby exerting potent anti-*Salmonella* activity.

RO interfered with the lipid metabolism and purine metabolism of Salmonella

Building on the previous findings, metabolomics analysis was employed to further elucidate the antibacterial mechanism of RO on *Salmonella*. Principal component analysis (PCA) revealed a significant difference in metabolites between SL1344 treated with MIC-level RO and untreated controls (Fig. 4A). Volcano plot and cluster analyses showed that, compared to untreated SL1344, RO-treated SL1344 exhibited a significant upregulation of 174 metabolites and a

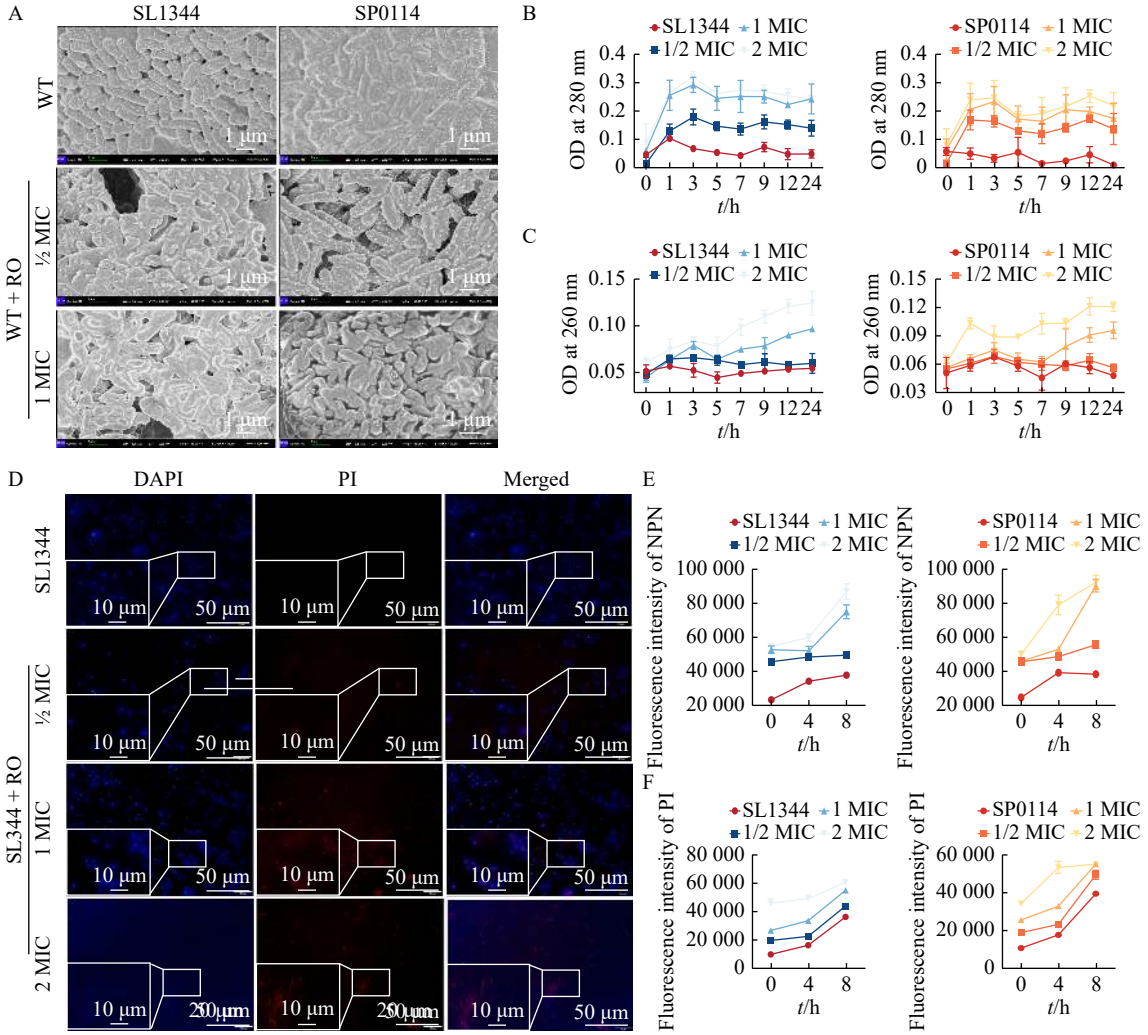

Fig. 2 RO damaged the cell membrane homeostasis of *Salmonella*. (A) SEM for the observation of SL1344 and SP0114 treated with RO. (B) Protein leakage analysis by monitoring the absorbance at 280 nm of SL1344 (left) and SP0114 (right) treated with 0, ½ MIC, MIC, and 2 × MIC RO at 0, 1, 3, 5, 7, 9, 12, and 24 h. (C) Nucleic acid leakage of SL1344 (left) and SP0114 (right) with the above treatments by monitoring the absorbance at 260 nm at the indicated time points. (D) DAPI/PI staining for SL1344 treated with RO. All bacteria were stained with DAPI (blue fluorescence) and PI (red fluorescence). (E) The fluorescence intensity of NPN was read at 0, 4, and 8 h in SL1344 (left) and SP0114 (right) with above treatments. (F) The fluorescence intensity of PI was read at 0, 4, and 8 h in SL1344 (left) and SP0114 (right) treated with above treaments.

downregulation of 34 metabolites (Figs. 4B and 4E). Following RO treatment, there was a marked increase in lipid metabolites (Fig. 4C). Additionally, KEGG enrichment analysis identified two significantly impacted pathways: lipid metabolism (P = 0.01) and purine metabolism (P = 0.006) (Fig. 4D). In the RO-treated SL1344 group, metabolites such as prostaglandin, arachidonate, and thromboxane B2 were enriched in the lipid metabolism pathway (Supplement Figs. 2A−2E). Meanwhile, metabolites, including inosinic acid, dADP, AMP, GMP, and ADP-ribose were enriched in the purine metabolism pathway (Supplement Figs. 2F−2O). Furthermore, the expression of purine metabolism-related upstream genes (*purF*, *purD*, *purK*, *purE*, *purH*) was significantly activated in the RO-treated SL1344 group (Supplement Figs. 3A−3E). Additionally, an increase in H_2O_2 levels and a decrease in hydroxyl free radical scavenging activity were observed in *Salmonella* treated with RO (Supplement Figs. 3F−3G). This oxidative stress is likely a consequence of the activation of lipid metabolism, as indicated by the KEGG pathway analysis.

RO provided systemic protection against Salmonella infection in vivo

To evaluate the therapeutic effect of RO *in vivo*, we investigated its ability to protect mice and chicks infected with *Salmonella typhimurium* SL1344 and *Salmonella pullorum* SP0114, respectively. The establishment of these infection models is illustrated in Fig. 5A and Supplement Fig. 4A. Following RO treatment, the liver index in infected mice and chicks was significantly reduced, while the indices of the cecum and colon increased (Fig. 5B and Supplement Fig. 4B). Untreated mice and chicks exhibited severe damage to multiple organs, whereas RO-treated animals showed allevi-

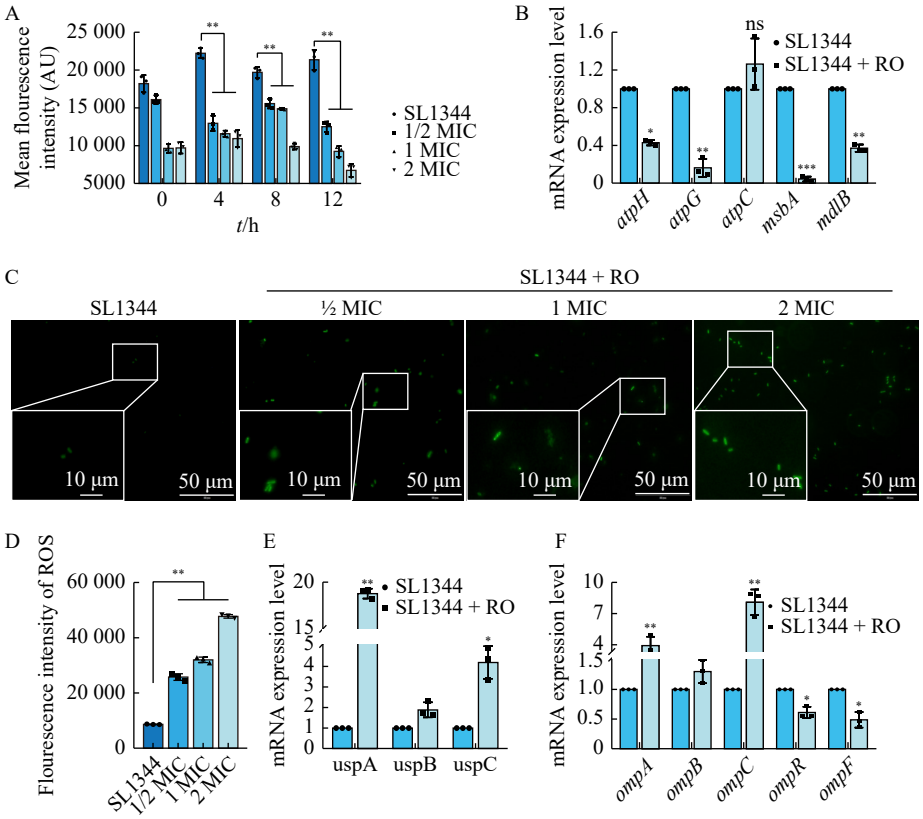

Fig. 3 The disruption of intracellular metabolic homeostasis of *Salmonella* by RO. (A) ATP levels in *Salmonella* at 0, 4, 8 and 12 h with the indicated concentrations of RO. (B) The transcription of ATP-related genes in *Salmonella* with or without MIC RO treatment by qRT-PCR analysis. (C) Fluorescence observation of intracellular ROS production in *Salmonella* in the presence of 0, ½ MIC, MIC, and 2 × MIC RO. The images are shown at 600 × magnification. (D) The fluorescence intensity of ROS in *Salmonella* was quantitatively evaluated under a microplate reader. qRT-PCR analysis for determination of the transcription of ROS-related genes (E) and *Omp*-related genes (F) in *Salmonella* with or without MIC RO treatment. Data are presented as the mean ± SD ($n = 3$), and *gyrB* was used as the internal reference for the qRT-PCR analysis in Panels B, E, and F. Statistically significant differences are shown between the samples treated with or without RO. $^{*}P < 0.05$; $^{**}P < 0.01$.

ated pathological damage both macroscopically and microscopically (Figs. 5C and 5D, Supplement Figs. 4C and 4D). The high dose of RO provided the most effective protection among the doses tested (Figs. 5C and 5D). RO treatment also reversed the decreases in daily weight, diet, and water intake caused by *Salmonella* infection in mice and chicks (Figs. 5E and 5G and Supplement Figs. 4E and 4G). Although low doses of RO did not significantly affect the bacterial load in the target organs of infected models, middle and high doses of RO significantly reduced the bacterial load (Fig. 5H and Supplement Fig. 4H). Notably, the number of bacterial colonies in the liver and colon of the high-dose group was reduced by almost 100-fold. The anti-colonization effect in organs was dependent on the RO dose (Fig. 5H). In summary, our results demonstrate that RO provides effective, dose-dependent protection against *Salmonella* infection in mice and chicks.

RO reduced Salmonella-mediated inflammation by inhibiting the MAPK/NF-κB pathway

To investigate the anti-inflammatory effects of RO in *Salmonella*-infected hosts, we measured inflammatory markers in target organs. In the control group, proinflammatory factors such as TNF-α (Fig. 6A), IL-1β (Fig. 6B), IL-6 (Fig. 6C), and IFN-γ (Fig. 6D and Supplement Fig. 5D) were significantly elevated due to *Salmonella* infection, while the anti-inflammatory factor IL-10 (Fig. 6E) was notably reduced. RO treatment effectively decreased the levels of these proinflammatory factors (Figs. 6A−6D) and increased the IL-10 levels (Fig. 6E). Further analysis of liver tissue revealed elevated expression levels of genes associated with the MAPK pathway (*JNK*, *ERK*, *p38*) and RPS3/NF-κB pathway in SL1344 or SP0114-infected mice or chicks (Figs. 6F−6G and Supplement Figs. 5B−5E). Additionally, the phosphorylated protein expression of the MAPK and NF-κB pathways was increased in infected liver tissue but decreased following RO treatment (Figs. 6I−6M). This indicates that RO inhibits the activation of these inflammatory pathways. The expression of proinflammatory genes in RO-treated mice was also significantly reduced, demonstrating RO's anti-inflammatory effect against *Salmonella* infection *in vivo* (Figs. 6F and 6G). In a lethal infection model, RO significantly increased both the survival rates and mid-term survival of infected mice and chicks, consistent with the previous results (Fig. 6H and Supplement Fig. 5F). Overall, our findings suggest that RO ad-

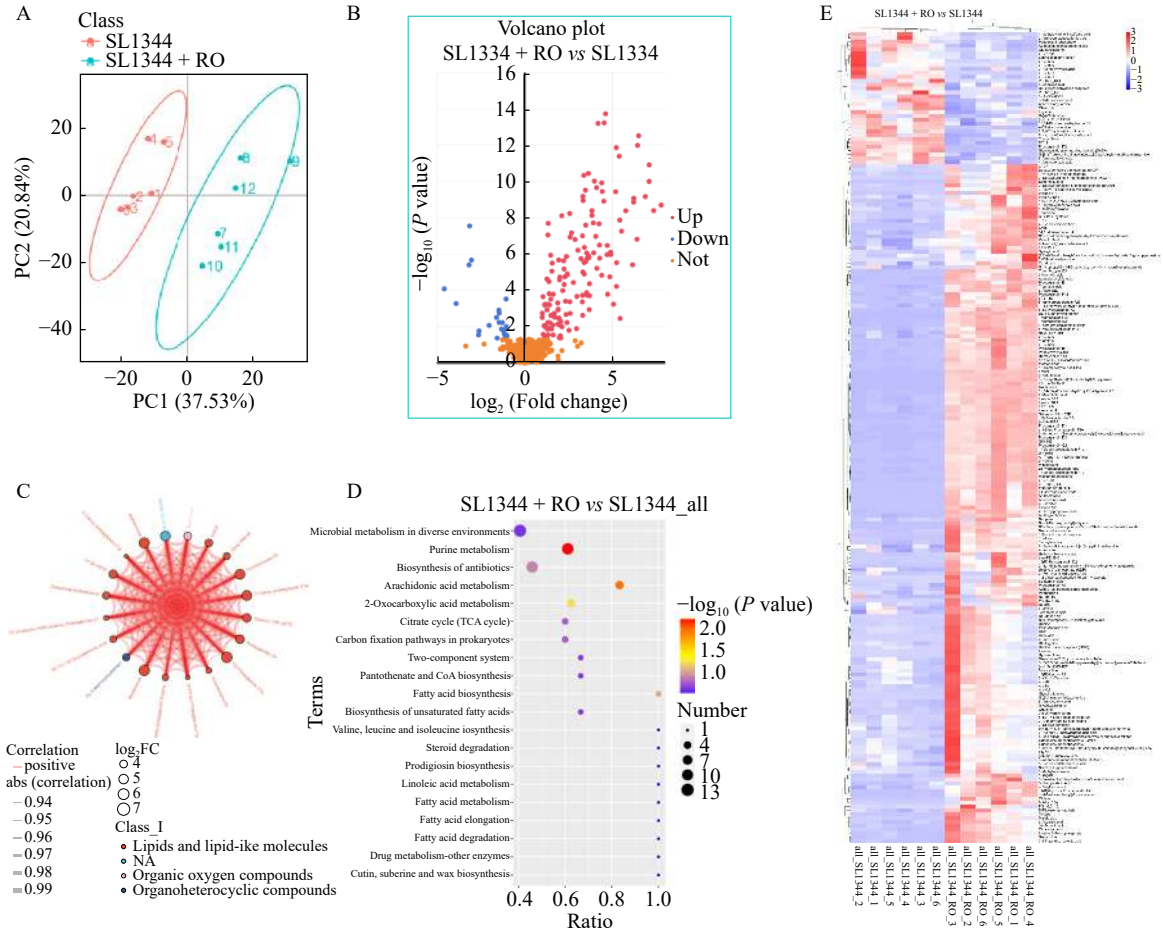

Fig. 4 Metabolomics analysis of *Salmonella* treated with or without RO. Metabolomic analysis (NEG and POS mode) of SL1344 treated with or without RO (n = 6). (A) PCA analysis of comparison in SL1344 with or without MIC RO. (B) Volcano chart analysis in the ALL mode of two groups. (C) Differential metabolite chord diagram of samples. (D) KEGG enrichment analysis of metabolic pathways of two groups. (E) Cluster analysis in POS mode of SL1344 with or without MIC RO. The x-axes and y-axes represent the different experimental groups and the different metabolites, respectively.

ministration to *Salmonella*-infected mice and chicks reduces the host inflammatory response and enhances survival rates by inhibiting the MAPK/NF-κB pathway.

Discussion

Foodborne diseases and severe environmental pollution caused by *Salmonella* continue to pose urgent global challenges [24]. The development of new antibiotics targeting *Salmonella* has stagnated, and antibiotic resistance in pathogenic bacteria is becoming increasingly problematic [25, 26]. This study aimed to explore NPs as alternative antimicrobial agents for the prevention and treatment of *Salmonella* infections. RO, derived from the traditional medicine *Aniba rosaeodora*, was found to be rich in linalool and identified as a promising antibacterial agent against various *Enterobacteriaceae* and *Staphylococcus aureus*. RO treatment provided systemic protection against *Salmonella* infection in both mice and chicks.

Beyond targeting bacterial virulence factors [27], RO disrupted cell membranes, leading to the leakage of intracellular substances in *Salmonella*. The germicidal curve and live/dead bacteria staining indicated that RO had an initial inhibitory effect on *Salmonella* at a 1 × MIC concentration and a bactericidal effect at a 2 × MIC concentration (Fig. 1). SEM observations revealed increased morphological damage to the cell membranes of *Salmonella* treated with RO (Fig. 2A). Additionally, the fluorescence intensity of NPN and PI in RO-treated *Salmonella* increased in a dose-dependent manner (Figs. 2E−2F), and significant leakage of proteins and nucleic acids was detected (Figs. 2C−2D). These findings suggest that RO damages bacterial membranes, causing the leakage of intracellular substances.

The Omp family, a key component of *Salmonella's* membrane channels, is crucial for maintaining membrane integrity and selective permeability [28]. *OmpA*, *ompB*, and *ompC* are notable transmembrane proteins essential for preserving membrane integrity and cell morphology [29, 30]. Conversely, overexpression of *OmpR* can reduce pore proteins and decrease sensitivity to certain drugs [31]. Our study found that the expression of *ompA*, *ompB*, and *ompC* increased in *Salmonella* treated with RO (Fig. 3F), likely due to an activated defense mechanism in response to RO. The decreased

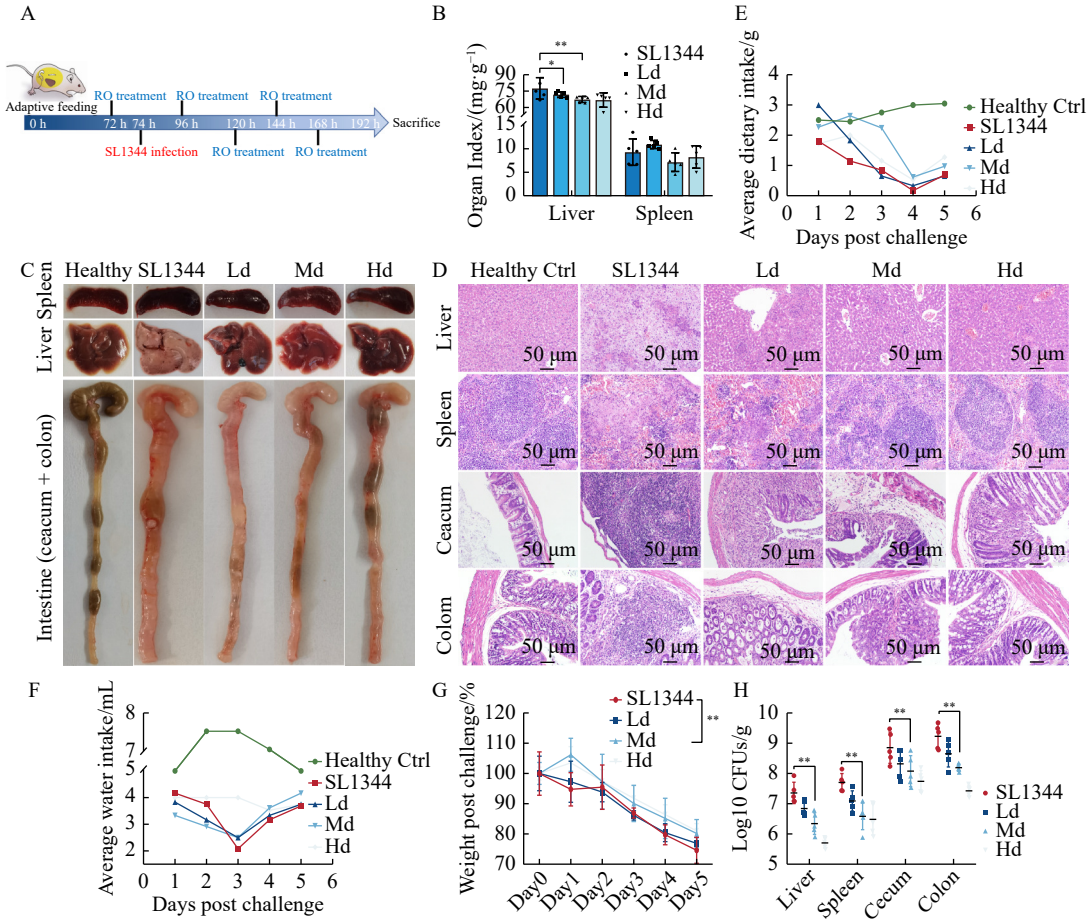

Fig. 5 RO treatment conferred systemic protection against SL1344 infection in mice. (A) Infection schematic for the SL1344-infected models in BALB/c female mice. Each mouse was inoculated with 1 × 10^7 CFUs of SL1344 and treated with 0 (SL1344), 40 (Ld), 80 (Md) or 160 (Hd) mg·kg^{-1}·d^{-1} RO or vehicle (0.5% CMC) for 5 d. (B) Organ index of the livers and spleens in the infected mice. (C) Gross observation of the livers, spleens, caecums, and colons from the infected mice. (D) HE staining analysis of target organs. Images are shown at 20 × magnification. Average dietary intake (E), water intake (F), and weight (G) of the infected mice for 5 d. (H) Inhibition of bacterial burden in target organs from the infected mice with RO treatment (n = 5). Statistically significant differences are shown between the samples. $^{*}P < 0.05$; $^{**}P < 0.01$.

expression of *ompR* and *ompF* suggests that RO inhibits the overexpression of *ompR*, preventing a reduction in pore proteins and facilitating RO entry through membrane pores, thus causing bacterial damage. This indicates that bacteria may upregulate certain *omp* genes to maintain survival when membrane functions are compromised by RO [32].

ATP and ROS are indispensable for bacterial metabolism and survival [33, 34]. Our research observed a depletion of ATP and excessive production of ROS in *Salmonella* treated with RO (Fig. 3A and 3D). The expression of ATP-related genes *atpH*, *atpG*, *msbA*, and *mdlB* was significantly reduced in RO-treated *Salmonella* (Fig. 3B), suggesting that RO restricts substrate transport mediated by cell membrane transport proteins *via* ATP depletion. This also inhibits the overexpression of efflux pumps, which can lead to drug resistance [35]. ATP depletion is closely associated with membrane damage [36]. Additionally, RO increased the expression of universal stress protein (USP) [37]-related genes and led to ROS overproduction in *Salmonella* (Fig. 3E). These findings indicate that RO disrupts cell membrane transporter-related gene expression, leading to cell death through ATP depletion and ROS overproduction.

Arachidonic acid (AA) is an unsaturated fatty acid with various biological activities. Research by ZHANG suggests that AA is produced by bacteria under low-oxygen conditions [38]. Consistent with this, we observed increased levels of H_2O_2 and decreased scavenging activity of hydroxyl radicals (·OH) in S*almonella* treated with RO, likely due to AA activation as indicated by KEGG analysis (Supplement Figs. 2F−2G). We hypothesize that the metabolic enrichment of AA in RO-treated bacteria impairs their ability to scavenge free radicals, leading to ROS accumulation (Fig. 4D). Additionally, RO disrupted purine metabolism homeostasis, increasing the transcription of purine metabolism-related genes in *Salmonella* (Supplement Figs. 2A−2E). This imbalance can lead to an accumulation of metabolic products and significant ATP depletion [39]. Consequently, RO interferes with bacterial metabolic homeostasis, compromising their surviv-

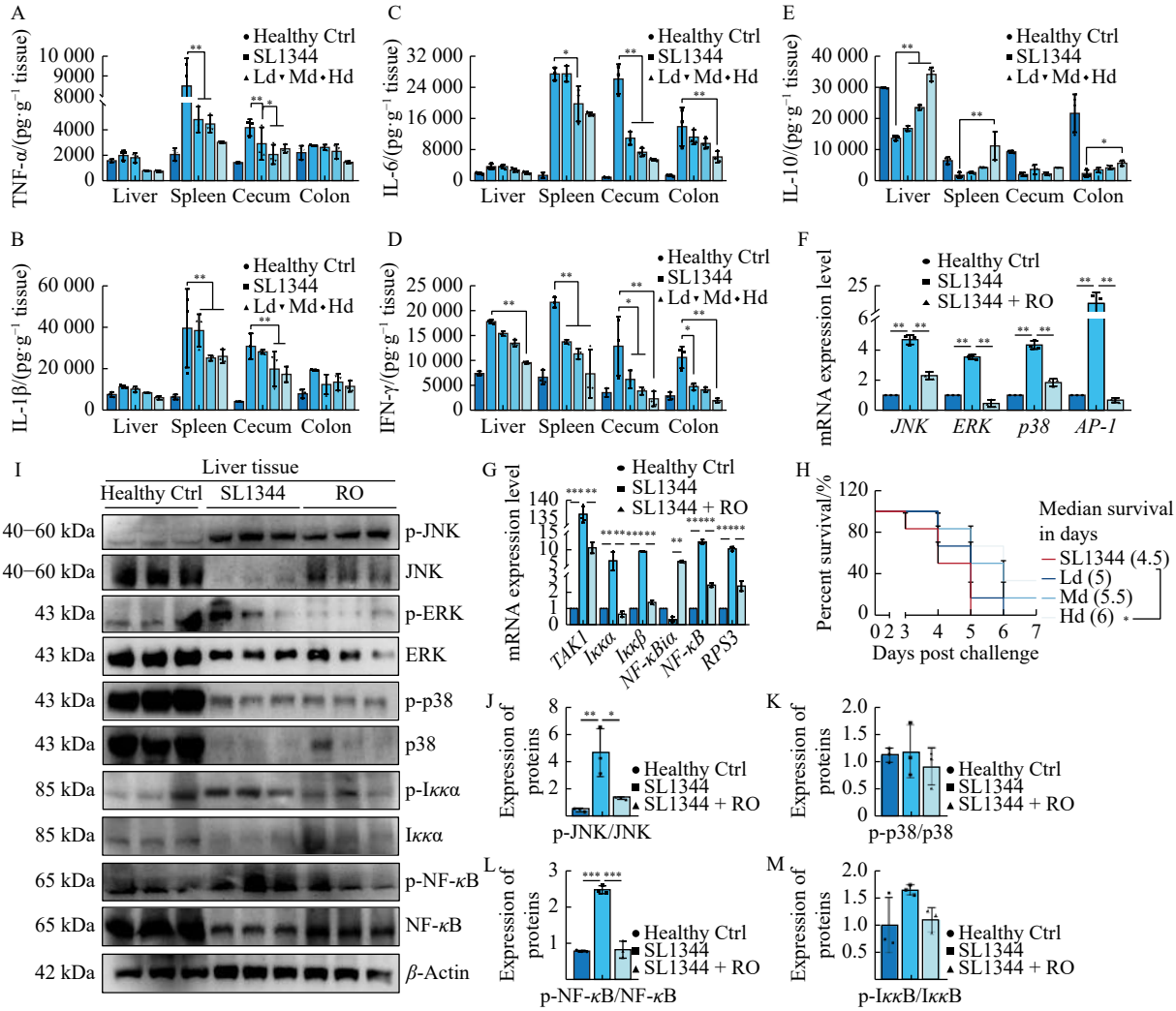

Fig. 6 RO reduced *Salmonella*-mediated inflammation by inhibiting the MAPK/NF-κB pathway. Mice infected with 1 × 10^7 CFUs of SL1344 were treated with 0 (SL1344), 40 (Ld), 80 (Md) or 160 (Hd) mg·kg^{-1}·d^{-1} RO or vehicle (0.5% CMC) for 5 d (n = 5). Then, the levels of inflammatory cytokines and the expression of signaling pathway-related genes were determined. TNF-α (A), IL-1β (B), IL-6 (C), IFN-γ (D) and IL-10 (E) were released from the livers, spleens, caecums, and colons of infected mice. Expression of (F) MAPK pathway-related genes (*JNK*, *ERK*, *p38* and *AP-1*) and (G) NF-κB/RPS3 pathway-related genes (*TAK1*, *Iκκα*, *Iκκβ*, *NF-κBiα*, *NF-κB* and *RPS3*) in the livers of the infected mice that received 80 mg·kg^{-1} RO or vehicle. (H) Percent survival of the SL1344-infected mice that received above RO by inoculating a lethal dose (5 × 10^7 CFUs per mouse) (n = 6). (I–M) Expression of proteins of the MAPK pathway (JNK, p-JNK, ERK, p-ERK, p38, p-p38) and NF-κB pathway (Iκκα, p-Iκκα, NF-κB-p65, p-NF-κB-p65) in the livers of the infected mice that received 80 mg·kg^{-1} RO or vehicle. β-Actin was used as the internal reference for the protein expression analysis in both panels J to M. Data are presented as the mean ± SD. Statistically significant differences are shown between the samples. $^*P < 0.05$; $^{**}P < 0.01$.

al by disrupting essential biosynthetic processes.

Host-directed therapy (HDT) is an alternative approach to treating bacterial infections [40]. Previous research demonstrated that essential oil from *Lippia* species inhibited the yellow fever virus in Vero cells [41]. Moreover, *in vivo* studies by Andrea Bonetti *et al*. showed that thyme essential oil maintained epithelial integrity, thereby reducing *E. coli* infection [42]. Our study demonstrated that RO effectively inhibited *Salmonella*-mediated MAPK/NF-κB activation and inflammatory responses in both mice and chicks (Figs. 6A–6I and supplement Fig. 5). Based on its protective effects and anti-*Salmonella* activity, we confirmed that RO provides systemic protection in experimental mice and target animal chicks.

Conclusion

In summary, our study elucidated the antibacterial mechanisms of RO and successfully established *Salmonella* infection models in chicks and mice to assess the anti-inflammatory effects of RO *in vivo*. Our findings demonstrate that RO disrupts bacterial membrane structures, thereby impairing the bacteria's ability to eliminate hydroxyl radicals (·OH) and promoting intracellular ROS production through the activation of lipid metabolism. By interfering with purine metabolism, RO causes an imbalance in bacterial metabolic pro-

cesses, leading to ATP depletion and ROS overproduction. This disruption results in the leakage of intracellular contents, including nucleic acids and proteins. Additionally, RO provided effective protection against *Salmonella* infection in both mice and chicks, reducing *Salmonella*-induced inflammation *via* the MAPK/RPS3/NF-*κ*B pathway. From a molecular biology perspective, we elucidated the anti-*Enterobacteriaceae* and protective effects of RO on target animals, highlighting its potential clinical application as a natural antibacterial compound. Our findings provide a theoretical basis for enhancing livestock breeding and protection and offer a viable reference for the clinical treatment of *Enterobacteriaceae* infections.

Supporting Information

Supporting information can be requested by sending E-mails to the corresponding authors.

References

[1] Majowicz SE, Musto J, Scallan E, *et al*. The global burden of nontyphoidal *Salmonella gastroenteritis* [J]. *Clin Infect Dis*, 2010, **50**(6): 882-889.

[2] Zhang JF, Fang LX, Chang MX, *et al*. A trade-off for maintenance of multidrug-resistant IncHI2 plasmids in *Salmonella enterica* serovar typhimurium through adaptive evolution [J]. *mSystems*, 2022, **7**(5): e0024822.

[3] Huang J, Liang L, Cui K, *et al*. *Salmonella* phage CKT1 significantly relieves the body weight loss of chicks by normalizing the abnormal intestinal microbiome caused by hypervirulent *Salmonella Pullorum* [J]. *Poult Sci*, 2022, **101**(3): 101668.

[4] Cardetti M, Rodríguez S, Sola A, *et al*. Use (and abuse) of antibiotics in perinatal medicine [J]. *An Pediatr (Engl Ed)*, 2020, **93**(3): 207.e1.

[5] Mcewen SA, Collignon PJ. Antimicrobial resistance: a one health perspective [J]. *Microbiol Spectr*, 2018, **6**(2): ARBA-0009-2017.

[6] Kumar A, Kumar A. Antibiotic resistome of *Salmonella typhi*: molecular determinants for the emergence of drug resistance [J]. *Front Med*, 2021, **15**(5): 693-703.

[7] Fan K, Zhang L, Tan B, *et al*. Antimicrobial indole alkaloids from *Tabernaemontana corymbosa* [J]. *Chin J Nat Med*, 2023, **21**(2): 146-153.

[8] Ulukanli Z, Karabörklü S, Bozok F, *et al*. Chemical composition, antimicrobial, insecticidal, phytotoxic and antioxidant activities of Mediterranean *Pinus brutia* and *Pinus pinea resin* essential oils [J]. *Chin J Nat Med*, 2014, **12**(12): 901-910.

[9] Anderson RC, Levent G, Petrujkić BT, *et al*. Antagonistic effects of lipids against the anti-*Escherichia coli* and anti-*Salmonella* activity of thymol and thymol-*β*-D-glucopyranoside in porcine gut and fecal cultures *in vitro* [J]. *Front Vet Sci*, 2021, **8**: 751266.

[10] Guo X, Hao Y, Zhang W, *et al*. Comparison of origanum essential oil chemical compounds and their antibacterial activity against *Cronobacter sakazakii* [J]. *Molecules*, 2022, **27**(19): 6702.

[11] Feng J, Lu M, Wang J, *et al*. Dietary oregano essential oil supplementation improves intestinal functions and alters gut microbiota in late-phase laying hens [J]. *J Anim Sci Biotechnol*, 2021, **12**(1): 72.

[12] Mathlouthi N, Bouzaienne T, Oueslati I, *et al*. Use of rosemary, oregano, and a commercial blend of essential oils in broiler chickens: *in vitro* antimicrobial activities and effects on growth performance [J]. *J Anim Sci*, 2012, **90**(3): 813-823.

[13] Baloch FS, Guizado SJV, Altaf MT, *et al*. Applicability of inter-primer binding site iPBS-retrotransposon marker system for the assessment of genetic diversity and population structure of Peruvian rosewood (*Aniba rosaeodora* Ducke) germplasm [J]. *Mol Biol Rep*, 2022, **49**(4): 2553-2564.

[14] De Sampaio LF, Maia JG, De Parijós AM, *et al*. Linalool from rosewood (*Aniba rosaeodora* Ducke) oil inhibits adenylate cyclase in the retina, contributing to understanding its biological activity [J]. *Phytother Res*, 2012, **26**(1): 73-77.

[15] Dos Santos ÉRQ, Maia CSF, Fontes Junior EA, *et al*. Linalool-rich essential oils from the Amazon display antidepressant-type effect in rodents [J]. *J Ethnopharmacol*, 2018, **212**: 43-49.

[16] De Siqueira RJ, Rodrigues KM, Da Silva MT, *et al*. Linalool-rich rosewood oil induces vago-vagal bradycardic and depressor reflex in rats [J]. *Phytother Res*, 2014, **28**(1): 42-48.

[17] Xu L, Lu G, Zhan B, *et al*. Uncovering the efficacy and mechanisms of *Genkwa flos* and bioactive ingredient genkwanin against *L. monocytogenes* infection [J]. *J Ethnopharmacol*, 2022, **297**: 115571.

[18] Li ZH, Cai M, Liu YS, *et al*. Antibacterial activity and mechanisms of essential oil from *Citrus medica* L. *var sarcodactylis* [J]. *Molecules*, 2019, **24**(8): 1577.

[19] Sheng Q, Hou X, Wang Y, *et al*. Naringenin microsphere as a novel adjuvant reverses colistin resistance *via* various strategies against multidrug-resistant *Klebsiella pneumoniae* infection [J]. *J Agric Food Chem*, 2022, **70**(51): 16201-16217.

[20] Murugan R, Rajesh R, Seenivasan B, *et al*. Withaferin A targets the membrane of *Pseudomonas aeruginosa* and mitigates the inflammation in zebrafish larvae; an *in vitro* and *in vivo* approach [J]. *Microb Pathog*, 2022, **172**: 105778.

[21] Wang X, Shen Y, Thakur K, *et al*. Antibacterial activity and mechanism of ginger essential oil against *Escherichia coli* and *Staphylococcus aureus* [J]. *Molecules,* 2020, **25**(17): 3955.

[22] Martínez SR, Durantini AM. Revealing ROS production by antibiotics and photosensitizers in biofilms: a fluorescence microscopy approach [J]. *Methods Mol Biol*, 2021, **2202**: 125-135.

[23] Lv Q, Chu X, Yao X, *et al*. Inhibition of the type III secretion system by syringaldehyde protects mice from *Salmonella enterica* serovar Typhimurium [J]. *J Cell Mol Med*, 2019, **23**(7): 4679-4688.

[24] Hu J, Xiao Y, Shao S A, *et al*. Construction and application of carbohydrate microarrays to detect foodborne bacteria [J]. *Chin J Nat Med*, 2020, **18**(3): 219-225.

[25] Peng S, Song D, Zhou B, *et al*. Persistence of *Salmonella typhimurium* and antibiotic resistance genes in different types of soil influenced by flooding and soil properties [J]. *Ecotoxicol Environ Saf*, 2022, **248**: 114330.

[26] Guo HX, Huang CY, Yan ZY, *et al*. New furo[3, 2-h]isochroman from the mangrove endophytic fungus *Aspergillus* sp. 085242 [J]. *Chin J Nat Med*, 2020, **18**(11): 855-859.

[27] Fekry M, Yahya G, Osman A, *et al*. GC-MS analysis and microbiological evaluation of caraway essential oil as a virulence attenuating agent against *Pseudomonas aeruginosa* [J]. *Molecules*, 2022, **27**(23): 8532.

[28] Reddy PN, Makam SS, Kota RK, *et al*. Functional characterization of a broad and potent neutralizing monoclonal antibody directed against outer membrane protein (OMP) of *Salmonella typhimurium* [J]. *Appl Microbiol Biotechnol*, 2020, **104**(6): 2651-2661.

[29] Yu S, Yan L, Wu X, *et al*. Multiplex PCR coupled with propidium monoazide for the detection of viable *Cronobacter sakazakii*, *Bacillus cereus*, and *Salmonella* spp. in milk and milk products [J]. *J Dairy Sci*, 2017, **100**(10): 7874-7882.

[30] Valero-Pacheco N, Blight J, Aldapa-Vega G, *et al*. Conserva-

tion of the OmpC porin among typhoidal and non-typhoidal *Salmonella* Serovars [J]. *Front Immunol*, 2019, **10**: 2966.
[31] Ko D, Choi SH. Mechanistic understanding of antibiotic resistance mediated by EnvZ/OmpR two-component system in *Salmonella enterica* serovar Enteritidis [J]. *J Antimicrob Chemother*, 2022, **77**(9): 2419-2428.
[32] Toobak H, Rasooli I, Talei D, *et al*. Immune response variations to *Salmonella enterica* serovar Typhi recombinant porin proteins in mice [J]. *Biologicals*, 2013, **41**(4): 224-230.
[33] Lee EJ, Groisman EA. Control of a *Salmonella* virulence locus by an ATP-sensing leader messenger RNA [J]. *Nature*, 2012, **486**(7402): 271-275.
[34] Noster J, Persicke M, Chao TC, *et al*. Impact of ROS-induced damage of TCA cycle enzymes on metabolism and virulence of *Salmonella enterica* serovar Typhimurium [J]. *Front Microbiol*, 2019, **10**: 762.
[35] Chen S, Cui S, Mcdermott PF, *et al*. Contribution of target gene mutations and efflux to decreased susceptibility of *Salmonella enterica* serovar Typhimurium to fluoroquinolones and other antimicrobials [J]. *Antimicrob Agents Chemother*, 2007, **51**(2): 535-542.
[36] Zhang J, Cui X, Zhang M, *et al*. The antibacterial mechanism of perilla rosmarinic acid [J]. *Biotechnol Appl Biochem*, 2022, **69**(4): 1757-1764.
[37] Raspoet R, Gantois I, Devloo R, *et al*. *Salmonella enteritidis* universal stress protein (usp) gene expression is stimulated by egg white and supports oviduct colonization and egg contamination in laying hens [J]. *Vet Microbiol*, 2011, **153**(1-2): 186-190.
[38] Zhang H, Feng Y, Cui Q, *et al*. Expression of *Vitreoscilla* hemoglobin enhances production of arachidonic acid and lipids in *Mortierella alpina* [J]. *BMC Biotechnol*, 2017, **17**(1): 68.
[39] Hershey AD, Dixon J, Chase M. Nucleic acid economy in bacteria infected with bacteriophage T2. I. Purine and pyrimidine composition [J]. *J Gen Physiol*, 1953, **36**(6): 777-789.
[40] Wang S, Lei P, Feng Y, *et al*. Jinyinqingre Oral Liquid alleviates LPS-induced acute lung injury by inhibiting the NF-κB/NLRP3/GSDMD pathway [J]. *Chin J Nat Med*, 2023, **21**(6): 423-435.
[41] Wani AR, Yadav K, Khursheed A, *et al*. An updated and comprehensive review of the antiviral potential of essential oils and their chemical constituents with special focus on their mechanism of action against various influenza and coronaviruses [J]. *Microb Pathog*, 2021, **152**: 104620.
[42] Bonetti A, Piva A, Grilli E, *et al*. Botanicals as a zinc oxide alternative to protect intestinal cells from an *Escherichia coli* F4 infection *in vitro* by modulation of enterocyte inflammatory response and bacterial virulence [J]. *Front Vet Sci*, 2023, **10**: 1141561.

Cite this article as: WANG Lanqiao, FANG Juan, WANG Heng, *et al*. Natural medicine can substitute antibiotics in animal husbandry: protective effects and mechanisms of rosewood essential oil against *Salmonella* infection [J]. *Chin J Nat Med*, 2024, **22**(9): 785-796.